Electron swarm properties under the influence of a very strong attachment in SF_6 and CF_3I obtained by Monte Carlo rescaling procedures

2016 Plasma Sources Sci. Technol. 25 065010

(http://iopscience.iop.org/0963-0252/25/6/065010)

IOP Publishing Plasma Sources Science and Technology

Plasma Sources Sci. Technol. **25** (2016) 065010 (15pp) doi:10.1088/0963-0252/25/6/065010

Electron swarm properties under the influence of a very strong attachment in SF_6 and CF_3I obtained by Monte Carlo rescaling procedures

J Mirić[1], D Bošnjaković[1], I Simonović[1], Z Lj Petrović[1,2] and S Dujko[1]

[1] Institute of Physics, University of Belgrade, PO Box 68, 11080 Belgrade, Serbia
[2] Serbian Academy of Sciences and Arts, Knez Mihailova 35, 11001 Belgrade, Serbia

E-mail: sasa.dujko@ipb.ac.rs

Received 13 May 2016, revised 28 July 2016
Accepted for publication 19 September 2016
Published 14 October 2016

Abstract

Electron attachment often imposes practical difficulties in Monte Carlo simulations, particularly under conditions of extensive losses of seed electrons. In this paper, we discuss two rescaling procedures for Monte Carlo simulations of electron transport in strongly attaching gases: (1) discrete rescaling, and (2) continuous rescaling. The two procedures are implemented in our Monte Carlo code with an aim of analyzing electron transport processes and attachment induced phenomena in sulfur-hexafluoride (SF_6) and trifluoroiodomethane (CF_3I). Though calculations have been performed over the entire range of reduced electric fields E/n_0 (where n_0 is the gas number density) where experimental data are available, the emphasis is placed on the analysis below critical (electric gas breakdown) fields and under conditions when transport properties are greatly affected by electron attachment. The present calculations of electron transport data for SF_6 and CF_3I at low E/n_0 take into account the full extent of the influence of electron attachment and spatially selective electron losses along the profile of electron swarm and attempts to produce data that may be used to model this range of conditions. The results of Monte Carlo simulations are compared to those predicted by the publicly available two term Boltzmann solver BOLSIG+. A multitude of kinetic phenomena in electron transport has been observed and discussed using physical arguments. In particular, we discuss two important phenomena: (1) the reduction of the mean energy with increasing E/n_0 for electrons in SF_6 and (2) the occurrence of negative differential conductivity (NDC) in the bulk drift velocity only for electrons in both SF_6 and CF_3I. The electron energy distribution function, spatial variations of the rate coefficient for electron attachment and average energy as well as spatial profile of the swarm are calculated and used to understand these phenomena.

Keywords: Monte Carlo, electron transport, electron attachment, SF_6, CF_3I

(Some figures may appear in colour only in the online journal)

1. Introduction

Electron transport in strongly attaching gases has long been of interest, with applications in many areas of fundamental physics and technology. Electron attaching gases support key processes for plasma etching and cleaning in semiconductor fabrication [1, 2], high-voltage gas insulation [3] and particle detectors in high energy physics [4–6]. The importance of studies of electron attachment has also been recognized in other fields, including planetary atmospheres, excimer lasers, plasma medicine and lighting applications, as well as in life science for understanding radiation damage in biological matter.

The fundamental importance of electron attachment processes has led to many experimental and theoretical swarm studies. For some gases the cross sections for attachment may be very large resulting in a rapid disappearance of free electrons that greatly complicates the measurements of transport coefficients [1, 7–9]. The pioneering studies date back to the 1970s, and the well-known swarm method of deriving cross section for electron attachment developed by Christophorou and his co-workers [10]. According to this method, trace amounts of an electron attaching gas are mixed into the buffer gases, typically nitrogen to scan the lower mean energies and argon to scan the higher mean energies. This technique results in the removal of electrons without disturbing the electron energy distribution function. In such mixtures the losses depend only on the very small amount of the added gas and we may measure the density reduced electron attachment rate coefficient. Electron attachment cross sections can be determined by deconvoluting the mixture data, since the electron energy distribution function is a known function of E/n_0 as calculated for the pure buffer gas. Examples of this procedure are cross sections for electron attachment in SF_6 and SF_6-related molecules [11–15] as well as cross sections and rate coefficients for a range of fluorocarbons [1, 12, 16–18] and other relevant gases for applications [1, 19–22]. In addition to non-equilibrium data, there is a separate category of experiments, including flowing afterglow, the Cavalleri diffusion experiment [9, 23, 24], and others that provide attachment rates for thermal equilibrium (i.e. without an applied electric field). These may be taken at different temperatures, but the range of energies covered by this technique is very narrow. These two techniques have been used to evaluate the cross sections for SF_6 and CF_3I, always under the assumption that the effect of attachment is merely on the number of particles and not on any other swarm properties.

A thorough understanding of the influence of attachment on the drift and diffusion of the electrons provides information which could be used in analysis of kinetic phenomena in complex electronegative gases and related plasmas. The attachment cooling and heating [25, 26], negative absolute electron flux mobility [27, 60] and anomalous phase shifts of drift velocity in AC electric fields [28] are some examples of these phenomena in strongly attaching gases, which may not be trivially predicted on the basis of individual collision events and external fields. Negative differential conductivity (NDC) induced by 3-body attachment for lower E/n_0 and higher pressures in molecular oxygen and its mixture with other gases is another example of phenomena induced by strong electron attachment [29]. The duality in transport coefficients, e.g. the existence of two fundamentally different families of transport coefficients, the bulk and flux, is caused by the explicit effects of electron impact ionization and electron attachment [7, 30–32]. The differences between two sets of data vary from a few percents to a few orders of magnitude and hence a special care is needed in the implementation of data in fluid models of plasma discharges [7, 31, 33–35]. On one hand, most plasma modeling is based on flux quantities while experiments aimed at yielding cross section data provide mostly but not uniquely the bulk transport data. This differentiation between flux and bulk transport properties is not merely a whimsy of theorists, but it is essential in obtaining and applying the basic swarm data. In addition, the production of negative ions has a large effect on the transport and spatial distribution of other charged particle species as well as on the structure of the sheath and occurrence of relaxation oscillations in charged particle densities [36–41].

There are three main approaches to the theoretical description of electron transport in gases: the kinetic Boltzmann equation, the stochastic particle simulation by the Monte Carlo method and semi-quantitative momentum transfer theory. Restrictions on the accuracy of momentum transfer theory for studies of electron transport in attaching gases, particularly under non-hydrodynamic conditions, have already been discussed and illustrated [31, 42, 43]. Boltzmann equation analyses for SF_6 and its mixtures with other gases (see for example [11, 44–50]) have been performed several times in the past. Two important studies devoted to the calculation of electron swarm parameters based on a Boltzmann equation have also been performed for CF_3I [51, 52]. Theories for solving the Boltzmann equation were usually restricted to low-order truncations in the Legendre expansions of the velocity dependence assuming quasi-isotropy in velocity space. The explicit effects of electron attachment were also neglected and electron transport was studied usually in terms of the flux data only. These theories had also restricted domains of validity on the applied E/n_0 in spite of their coverage of a considerably broader range. One thing that strikes the reader surveying the literature on electron transport in SF_6 is the systematic lack of reliable data for electron transport coefficients for E/n_0 less than 50 Td. Contemporary moment methods for solving Boltzmann's equation [31, 53] are also faced with a lot of systematic difficulties, particularly under conditions of the predominant removal of the lower energy electrons which results in an increase in the mean energy, i.e. attachment heating. Under these conditions the bulk of the distribution function is shifted towards a higher energy which in turn results in the high energy tail falling off much slower than a Maxwellian. This is exactly what may happen in the analysis of electron transport in strongly attaching gases such as SF_6 or CF_3I for lower E/n_0. The moment method for solving Boltzmann's equation under these circumstances usually requires the prohibitive number of basis functions for resolving the speed/energy dependency of the distribution function and/or unrealistically large computation time. As a consequence, the standard numerical schemes employed within the framework of moment methods usually fail.

The present investigation is thus mainly concerned with the Monte Carlo simulations of electron transport in strongly attaching gases. Monte Carlo simulations have also been employed for the analysis of electron transport in the mixtures of SF_6 [46, 54–57] and CF_3I [58] with other gases usually with an aim of evaluating the insulation strength and critical electric fields. However, electron attachment in strongly electronegative gases often imposes practical difficulties in Monte Carlo simulations. This is especially noticeable at lower E/n_0, where electron attachment is one of the dominant processes which may lead to the extensive vanishing of the seed electrons and

consequently to the decrease of the statistical accuracy of the output results. In extreme cases, the entire electron swarm might be consumed by attachment way before the equilibrated (steady-state regime) is achieved. An obvious solution would be to use a very large number of initial electrons, but this often leads to a dramatic increase of computation time and/or required memory/computing resources which are beyond practical limits. Given the computation restrictions of the time, the workers were forced to develop methods to combat the computational difficulties induced by the extensive vanishing of the seed electrons. Two general methods were developed: (1) addition of new electrons by uniform scaling of the electron swarm at certain time instants under hydrodynamic conditions [26, 59] or at certain positions under steady-state Townsend conditions [60], when number of electrons reaches a pre-defined threshold, and (2) implementation of an additional fictitious ionization channel/process with a constant collision frequency (providing that the corresponding ionization rate is chosen to be approximately equal to the attachment rate) [54]. On the other hand, similar rescaling may be applied for the increasing number of electrons as has been tested at the larger E/n_0 by Li *et al* [61]. Further distinction and specification between methods developed by Nolan *et al* [26] and Dyatko *et al* [60] on one hand and Raspopović *et al* [59] on the other, will be discussed in later sections. These methods have not been compared to each other in a comprehensive and rigorous manner. This raises a number of questions. How accurate, these methods are? Which is the more efficient? Which is easier for implementation? What is their relationship to each other? Which one is more flexible? In this paper, we will try to address some of these issues. In particular, the present paper serves to summarize the salient features of these methods in a way which we hope will be of benefit to all present and future developers of Monte Carlo codes. Finally, it is also important to note that in the present paper we extend the method initially developed by Yousfi *et al* [54], by introducing time-dependent collision frequency for the fictitious ionization process.

This paper is organized as follows: in section 2, we briefly review the basic elements of our Monte Carlo code, before detailing the rescaling procedures employed to combat the computational difficulties initiated by the rapid disappearance of electrons. In the same section, we illustrate the issue of electron losses by considering the evolution of the number of electrons for a range of E/n_0 in SF_6 and CF_3I. In section 3, we evaluate the performance of rescaling procedures by simulating electron transport in SF_6 and CF_3I over a wide range of E/n_0. We will also highlight the substantial difference between the bulk and flux transport coefficients in SF_6 and CF_3I. Special attention will be paid to the occurrence of negative differential conductivity (NDC) in the profile of the bulk drift velocity. For electrons in SF_6 another phenomenon arises: for certain reduced electric fields we find regions where the swarm mean energy decreases with increasing E/n_0. In the last segment of the section 3, we discuss two important issues: (1) how to use the rescaling procedures in Monte Carlo codes, and (2) rescaling procedures as a tool in the modeling of non-hydrodynamic effects in swarm experiments. In section 4, we present our conclusions and recommendations.

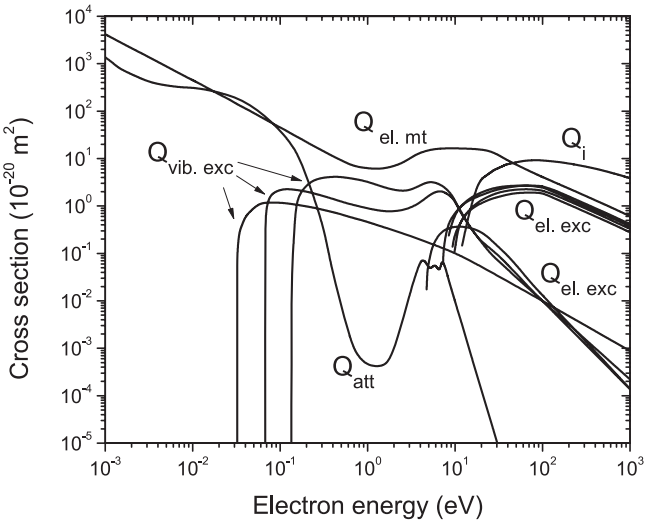

Figure 1. Electron impact cross-sections for CF_3I used in this study [62]: $Q_{el.\ mt}$ momentum transfer in elastic collisions, $Q_{vib.\ exc}$ vibrational excitation, $Q_{el.\ exc}$ electronic excitation, Q_{att} dissociative attachment and Q_i electron-impact ionization.

2. Input data and computational methods

2.1. Cross sections for electron scattering and simulation conditions

We begin this section with a brief description of cross sections for electron scattering in SF_6 and CF_3I. For the SF_6 cross sections we use the set developed by Itoh *et al* [47]. This set was initially based on published measurements of cross sections for individual collision processes. Using the standard swarm procedure, the initial set was modified to improve agreement between the calculated swarm parameters and the experimental values. The set includes one vibrational channel, one electronic excitation channel, as well as elastic, ionization and five different attachment channels.

This study considers electron transport in CF_3I using the cross section set developed in our laboratory [62]. This set of cross sections is shown in figure 1. It should be noted that this set is similar but not identical to that developed by Kimura and Nakamura [63]. We have used the measured data under pulsed Townsend conditions for pure CF_3I and its mixtures with Ar and CO_2 in a standard swarm procedure with the aim of improving the accuracy and completeness of a set of cross sections. It consists of the elastic momentum transfer cross section, three cross sections for vibrational and five cross sections for electronic excitations as well as one cross section for electron-impact ionization with a threshold of 10.4 eV and one cross section for dissociative attachment. For more details the reader is referred to our future paper [64].

For both SF_6 and CF_3I all electron scattering are assumed isotropic and hence the elastic cross section is the same as the elastic momentum transfer cross section. Simulations have been performed for E/n_0 ranging from 1 to 1000 Td. The pressure and temperature of the background gas are 1 Torr and 300 K, respectively. It should be mentioned that special care in our Monte Carlo code has been paid to proper treatment of the thermal motion of the host gas molecules and their influence

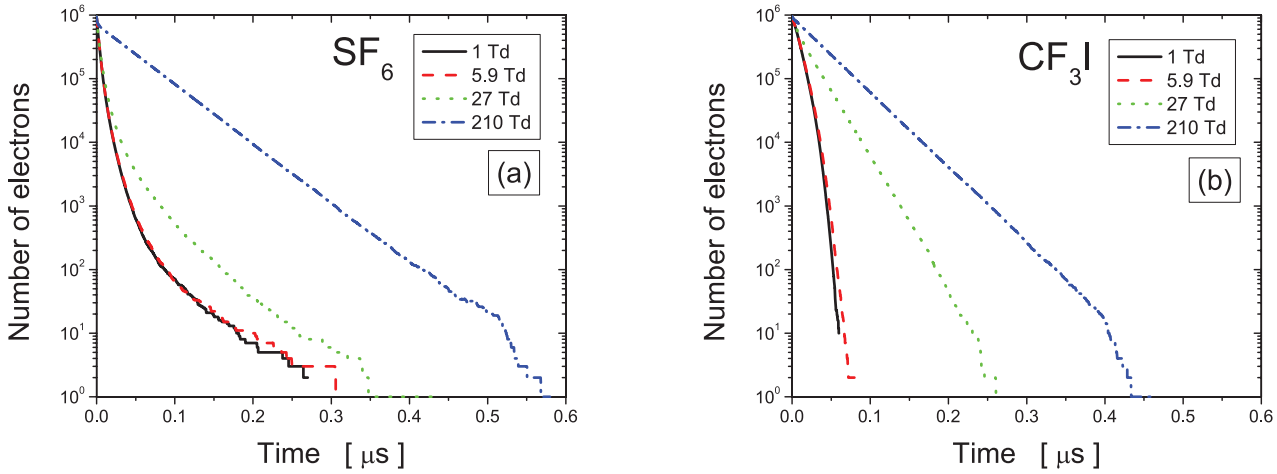

Figure 2. Electron number density decay for four different reduced electric fields as indicated on the graph. Calculations are performed for SF_6 (a) and CF_3I (b).

on electrons, which is very important at low electric fields, when the mean electron energy is comparable to the thermal energy of the host gas [65]. After ionization, the available energy is partitioned between two electrons in such a way that all fractions of the distribution are equally probable.

2.2. Monte Carlo method

The Monte Carlo simulation technique used in the present work is described at length in our previous publications [32, 53, 59, 66, 67]. In brief, we follow the spatiotemporal evolution of each electron through time steps which are fractions of the mean collision time. In association with random numbers, these finite time steps are used to solve the integral equation for the collision probability in order to determine the time of the next collision. The number of time steps is determined in such a way as to optimize the performance of the Monte Carlo code without reducing the accuracy of the final results. When the moment of the next collision is established, the additional sequences of random numbers are used, first to determine the nature of a collision, taking into account the relative probabilities of the various collision types, and second to determine the change in the direction of the electron velocity. All dynamic properties of each electron such as position, velocity, and energy are updated between and after the collisions. Sampling of electron dynamic properties is not correlated to the time of the next collision and is performed in a way that ensemble averages can be taken in both the velocity and configuration space. Explicit formulas for the bulk and flux transport properties have been given in our previous publications [59, 66]. To evaluate the accuracy of the Monte Carlo code, Boltzmann analyses were performed in parallel with the Monte Carlo calculations using the multi term method described in detail by Dujko *et al* [53]. In addition, we use the BOLSIG+, a publicly available Boltzmann solver based on a two term theory [68]. The most recent version of this code might be used to study the electron transport in terms of both the flux and bulk data which is very useful for some aspects of plasma modeling [7]. At the same time, the comparison between our results and those computed by BOLSIG+ which is presented in this paper, should be viewed as the first benchmark for the bulk BOLSIG+ data. Our Monte Carlo code and multi term codes for solving the Boltzmann equation have been subject of a detailed testing for a wide range of model and real gases [31, 53, 59, 67].

In figure 2 we illustrate the losses of electrons during the evolution of the swarm towards the steady-state. The initial number of electrons is set to 1×10^6 and calculations are performed for a range of reduced electric fields E/n_0 as indicated on the graphs. For both SF_6 and CF_3I, we observe that at small E/n_0, i.e. at low mean energies, the number of electrons decreases much faster. This is a clear sign that collision frequency for electron attachment increases with decreasing E/n_0. Electrons in CF_3I are lost continuously and consequently the number of electrons in the swarm decreases exponentially with time. The same trend may be observed for electrons in SF_6 at 210 Td. For the remaining E/n_0 the number of electrons is reduced with time even faster. Comparing SF_6 and CF_3I, it is evident that the electrons are more efficiently consumed by electron attachment in SF_6 in the early stage of the simulation. Conversely, in the last stage of simulation the electrons are more consumed by electron attachment in CF_3I than in SF_6. In any case, the electron swarms in both cases are entirely consumed by attachment way before the steady-state regime and hence the simulations are stopped. In other words, the number density drops down by six orders of magnitude over the course of several hundred nanoseconds in both gases. To facilitate the numerical simulation, it is clear that some kind of rescaling of the number density is necessary to compensate for the electrons consumed by electron attachment. This procedure should not in any way disrupt the spatial gradients in the distribution function. On the other hand, releasing electrons with some fixed arbitrary initial condition would require that they equilibrate with the electric field during which time again majority of such additional electrons would be lost.

2.3. Rescaling procedures

To counteract the effect of attachment in an optimal fashion while keeping the statistical accuracy, the following rescaling procedures were proposed and applied so far:

(1) Uniform generation of new electrons with initial properties taken from the remaining electrons thus taking advantage of the equilibration that has been achieved so far [59]. To make this procedure effective i.e. to avoid losing population in some smaller pockets of the ensemble the population should be allowed to oscillate between N_1 and N_0, where $N_1 > N_0$ but their difference is relatively small. Here N_0 is minimum allowed number of electrons while N_1 is maximum number of electrons in the simulation after rescaling.
(2) Uniform scaling of an electron swarm by a factor of 2 or 3 at certain instants of time [26] or distance [60] depending on the simulation conditions where the probability of scaling for each electron is set to unity.
(3) Introduction of an additional fictitious ionization process with a constant ionization frequency (that is close to the rate for attachment), which artificially increases the number of simulated electrons [54, 61]. Uniform rescaling of the swarm is done by randomly choosing the electrons which are to be 'duplicated'. The newborn electron has the same initial dynamic properties, coordinates, velocity, and energy as the original. Following the creation of a new electron their further histories diverge according to the independently selected random numbers.

Comparing the procedures (1) and (2), it is clear that there are no essential differences between them. The only difference lies in the fact that in the procedure (2) duplicating is performed for all the electrons in the simulation while according the procedure (1), the probability of duplication is determined by the current ratio of the number of electrons to the desired number of electrons in the simulation, which is specified in advance. On the other hand, fictitious ionization collision generates a new electron which is given the same position, velocity and energy as the primary electron that is not necessarily the electron lost in attachment. In this paper, we shall refer to the procedure (1) as *discrete rescaling*, since the procedure is applied at discrete time instants. The procedure (2) shall be termed as *swarm duplication* and finally we shall refer to the procedure (3) as the *continuous rescaling* since the rescaling is done during the entire simulation. An important requirement is that the rescaling must not perturb/change/disturb the normalized electron distribution function and its evolution. Li *et al* [61] showed that the continuous rescaling procedure meets this requirement. In case of discrete rescaling as applied to the symmetrical yet different problem of excessive ionization, it was argued that one cannot be absolutely confident that the rescaled distribution is a good representation of the original [69], except when steady state is achieved [70].

In what follows, we discuss the continuous rescaling. Following the previous works [54, 61], the Boltzmann equation for the distribution function $f(\mathbf{r}, \mathbf{c}, t)$ without rescaling and $f^\star(\mathbf{r}, \mathbf{c}, t)$ with rescaling are given by:

$$(\partial_t + \mathbf{c} \cdot \nabla_\mathbf{r} + \mathbf{a} \cdot \nabla_\mathbf{c}) f(\mathbf{r}, \mathbf{c}, t) = -J(f), \tag{1}$$

and

$$(\partial_t + \mathbf{c} \cdot \nabla_\mathbf{r} + \mathbf{a} \cdot \nabla_\mathbf{c}) f^\star(\mathbf{r}, \mathbf{c}, t) = -J(f^\star) + \nu_{\mathrm{fi}}(t) f^\star, \tag{2}$$

where $\mathbf{a}$ is the acceleration due to the external fields, $J(f)$ is the collision operator for electron-neutral collisions and ν_{fi} is time-dependent fictitious ionization rate. If the collision operator is linear (i.e. if electron–electron collisions are negligible) and if the initial distributions (at time $t = 0$) are the same, it can be easily shown that the following relationship holds

$$f^\star(\mathbf{r}, \mathbf{c}, t) = f(\mathbf{r}, \mathbf{c}, t) \exp\left(\int_0^t \nu_{\mathrm{fi}}(\tau) \mathrm{d}\tau \right). \tag{3}$$

Substituting equation (3) into equation (2) and using the linearity of the collision operator yields the following equation

$$J(f^\star) = \exp\left(\int_0^t \nu_{\mathrm{fi}}(\tau) \mathrm{d}\tau \right) J(f). \tag{4}$$

Note that in contrast to Li *et al* [61] the collision frequency for the fictitious ionization is now a time-dependent function. In terms of numerical implementation, the only difference between our continuous rescaling procedure and the one described in [54, 61] is that we do not need to provide the fictitious ionization rate which is estimated by trial and error, in advance (*a priori*). Instead, our fictitious ionization rate is initially chosen to be equal to the calculated attachment rate at the beginning of the simulation. Afterwards, it is recalculated at fixed time instants in order to match the newly developed attachment rates. As a result, the number of electrons during the simulation usually does not differ from the initial one by more than 10%. It should be noted that the fictitious ionization process must not in any way be linked to the process of real ionization. It was introduced only as a way to scale the distribution function, or in other words, as a way of duplicating the electrons.

3. Results and discussion

In this section the rescaling procedures and associated Monte Carlo code outlined in the previous section are applied to investigate transport properties and attachment induced phenomena for electrons in SF_6 and CF_3I. Electron transport in these two strongly attaching gases provides a good test of different rescaling procedures, particularly for lower E/n_0 where electron attachment is the dominant non-conservative process. In addition to comparisons between different rescaling procedures, the emphasis of this section is the observation and physical interpretation of the attachment induced phenomena in the E/n_0-profiles of mean energy, drift velocity and diffusion coefficients. In particular, we investigate the differences between the bulk and flux transport coefficients. We do not compare our results with experimentally measured data as it would distract the reader's attention to the problems associated with the quality of the sets of the cross sections for electron scattering. There are no new experimental measurements of transport coefficients for electrons in SF_6, particularly for E/n_0 less than 50 Td and thus we have deliberately chosen not to display the comparison. On the other hand, one cannot expect the multi term results to be useful here as the conditions with excessive attachment would make convergence difficult in the low E/n_0 region, where comparison would be of

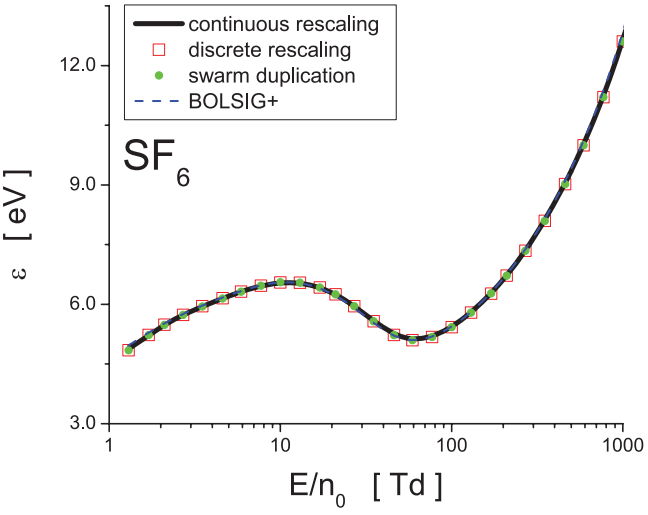

Figure 3. Variation of the mean energy with E/n_0 for electrons in SF_6. Monte Carlo results using three different techniques for electron number density compensation (rescaling) are compared with the BOLSIG+ results.

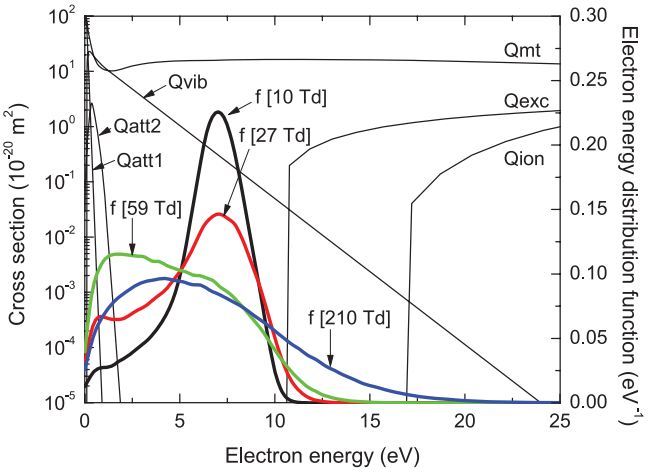

Figure 4. Electron energy distribution functions for E/n_0 of 10, 27, 59 and 210 Td. Cross sections for elastic momentum transfer (Qmt), electronic excitation (Qexc) and ionization (Qion) as well as for attachments that lead to the formation of SF_6^- (Qatt1) and SF_5^- (Qatt2) ions, are also included.

interest. Thus, for clarity the multi term results are omitted. Both experimental and theoretical work on electron swarms in SF_6 prior to 1990 is summarized in the papers of Phelps and van Brunt [11], Gallagher *et al* [71] and Morrow [72]. Recent results can be found in the book by Raju [22] and the review article of Christophorou and Olthoff [12]. The swarm analysis and further improvements of the cross sections for electron scattering in CF_3I is a subject of our future work [64].

3.1. Transport properties for electrons in SF_6 and CF_3I

3.1.1. Mean energy. In figure 3 we show the variation of the mean energy with E/n_0 for electrons in SF_6. The agreement between different rescaling procedures is excellent. This suggests that all rescaling procedures are equally valid for calculation of the mean energy (provided that rescaling is performed carefuly). In addition, the BOLSIG+ results agree very well with those calculated by a Monte Carlo simulation technique. For lower E/n_0, the mean energy initially increases with E/n_0, reaching a peak at about 10 Td, and then surprisingly it starts to decrease with E/n_0. The minimum of mean energy occurs at approximately 60 Td. For higher E/n_0 the mean energy monotonically increases with E/n_0. The reduction in the mean energy with increasing E/n_0 has been reported for electrons in Ar [73] and O_2 [74] but in the presence of very strong magnetic fields. In the present work, however, the mean energy is reduced in absence of magnetic field which certainly represents one of the most striking and anomalous effects observed in this study. Moreover, this behavior is contrary to previous experiences in swarm physics as one would expect the mean swarm energy to increase with increasing E/n_0. This is discussed in detail below.

In order to understand the anomalous behavior of the mean energy of electrons in SF_6, in figure 4 we display the electron energy distribution functions for E/n_0 at 10, 27, 59 and 210 Td. Cross sections for some of the more relevant collision processes are also included, as indicated in the graph. For clarity, the attachment cross sections for the formation of SF_4^-, F_2^- and F^- are omitted in the figure. For E/n_0 of 10 and 27 Td we observe the clear signs of 'hole burning' in the electron energy distribution function (EEDF). This phenomenon has been extensively discussed for electrons in O_2 [75, 76], O_2 mixtures [29, 77] and under conditions leading to the phenomenon of absolute negative electron mobility [27, 60] as well as for electrons in the gas mixtures of $C_2H_2F_4$, iso-C_4H_{10} and SF_6 used in resistive plate chambers in various high energy physics experiments at CERN [6]. For electrons in SF_6, the collision frequency for electron attachment decreases with energy and hence the slower electrons at the trailing edge of the swarm are preferentially attached. As a consequence, the electrons are 'bunched' in the high-energy part of the distribution function which in turn moves the bulk of the distribution function to higher energies. This is the well-known phenomenon of attachment heating which has already been discussed in the literature for model [25, 26] and real gases [6, 29]. In the limit of the lowest E/n_0 we see that due to attachment heating the mean energy attains the unusually high value of almost 5 eV. For a majority of molecular gases, however, the mean energy is significantly reduced for lower E/n_0 due to presence of rotational, vibrational and electronic excitations which have threshold energies over a wide range. As E/n_0 further increases the mean energy is also increased as electrons are accelerated through a larger potential. However, in case of SF_6, for E/n_0 increasing beyond 10 Td the mean energy is reduced. This atypical situation follows from the combined effects of attachment heating and inelastic cooling. From figure 4 we see that for E/n_0 of 27 and 59 Td the electrons from the tail of the corresponding distribution functions have enough energy to undergo the electronic excitation. Whenever an electron undergoes electronic excitations (or ionization) it loses the threshold energy of 9.8 eV (or 15.8 eV in case of ionization) and emerges from the collision with a reduced energy. This in turn diminishes the phenomenon of 'hole burning' in the distribution function by repopulating

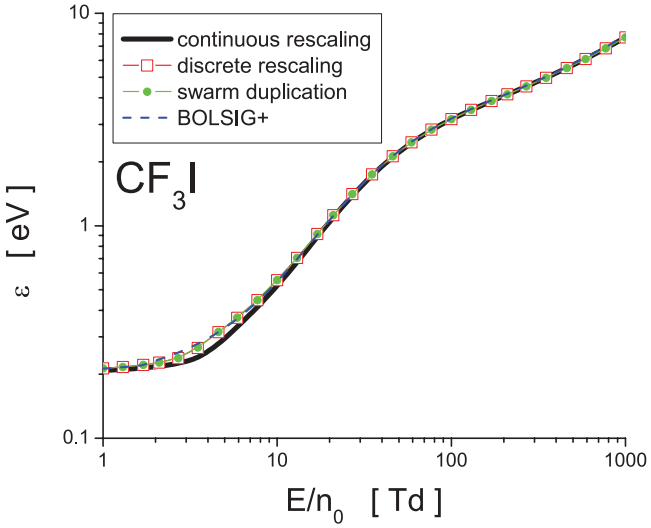

Figure 5. Variation of the mean energy with E/n_0 for electrons in CF_3I. Monte Carlo results using three different techniques for electron compensation are compared with the BOLSIG+ results.

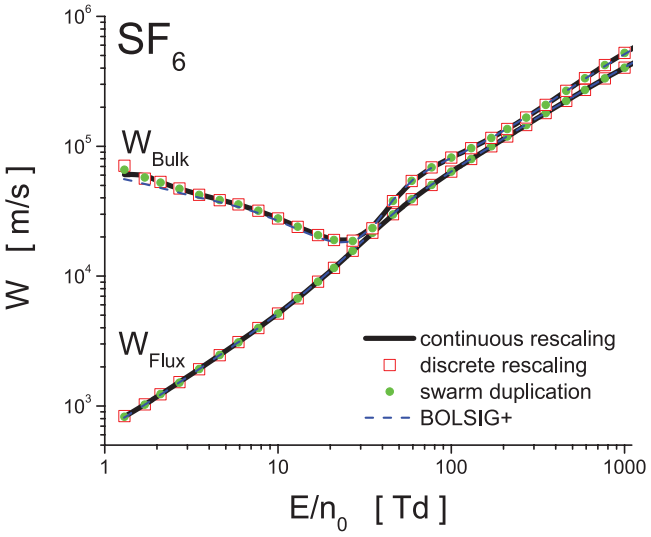

Figure 6. Variation of the drift velocity with E/n_0 for electrons in SF_6. Monte Carlo results using three different techniques for electron number density compensation are compared with the BOLSIG+ results.

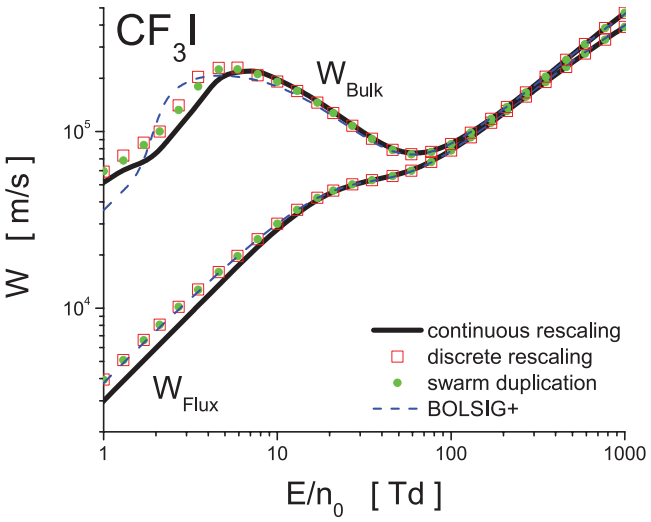

Figure 7. Variation of the drift velocity with E/n_0 for electrons in CF_3I. Monte Carlo results using three different techniques for electron number density compensation are compared with the BOLSIG+ results.

the distribution function at the lower energy. The combined effects of attachment heating and inelastic cooling and subsequent redistribution of low-energy electrons are more significant for the energy balance than the energy gain from electric field and losses in other collisions. The vibrational excitation with the threshold of 0.098 eV is of less importance having in mind the actual values of the mean energy. For E/n_0 higher than 60 Td, the dominant part in the energy balance is the energy gain from the electric field while attachment heating and induced phenomena are significantly suppressed. Thus, for E/n_0 higher than 60 Td the mean energy monotonically increases with increasing E/n_0.

The variation of the mean energy with E/n_0 for electrons in CF_3I is shown in figure 5. The agreement between different rescaling procedures is very good. Small deviations between discrete rescaling and swarm duplication from one side and continuous rescaling from the other side are present between approximately 3 and 20 Td. BOLSIG+ slightly overestimates the mean energy only in the limit of the lowest E/n_0. In contrast to mean energy of the electrons in SF_6, the mean energy of the electrons in CF_3I monotonically increases with E/n_0 without signs of anomalous behavior. If we take a careful look, then we can isolate three distinct regions of electron transport in CF_3I as E/n_0 increases. First, there is an initial region where the mean energy raises relatively slowly due to large energy loss of the electrons in low-threshold vibrational excitations. In this region the mean energy of the electrons is well above the thermal energy due to extensive attachment heating. The mean energy is raised much sharper between approximately 5 and 50 Td, indicating that electrons become able to overcome low-threshold vibrational excitations. The following region of slower rise follows from the explicit cooling of other inelastic processes, including electronic excitations and ionization, as these processes are now turned on. In conclusion, the nature of cross sections for electron scattering in CF_3I and their energy dependence as well as their mutual relations do not favor the development of the anomalous behavior of the swarm mean energy.

3.1.2. Drift velocity. In figures 6 and 7 we show variation of the bulk and flux drift velocity with E/n_0 for electrons in SF_6 and CF_3I, respectively. For electrons in SF_6 the agreement between different rescaling procedures for electron compensation is excellent for both the bulk and flux drift velocity over the entire E/n_0 range considered in this work. The BOLSIG+ bulk results slightly underestimate the corresponding bulk Monte Carlo results in the limit of the lowest E/n_0. For electrons in CF_3I, the agreement among different rescaling procedures for electron compensation is also good except for lower E/n_0 where the continuous rescaling gives somewhat lower results than other techniques.

For both SF_6 and CF_3I, we see that the bulk dominates the flux drift velocity over the entire E/n_0 range considered in this work. For lower E/n_0 this is a consequence of a very intense

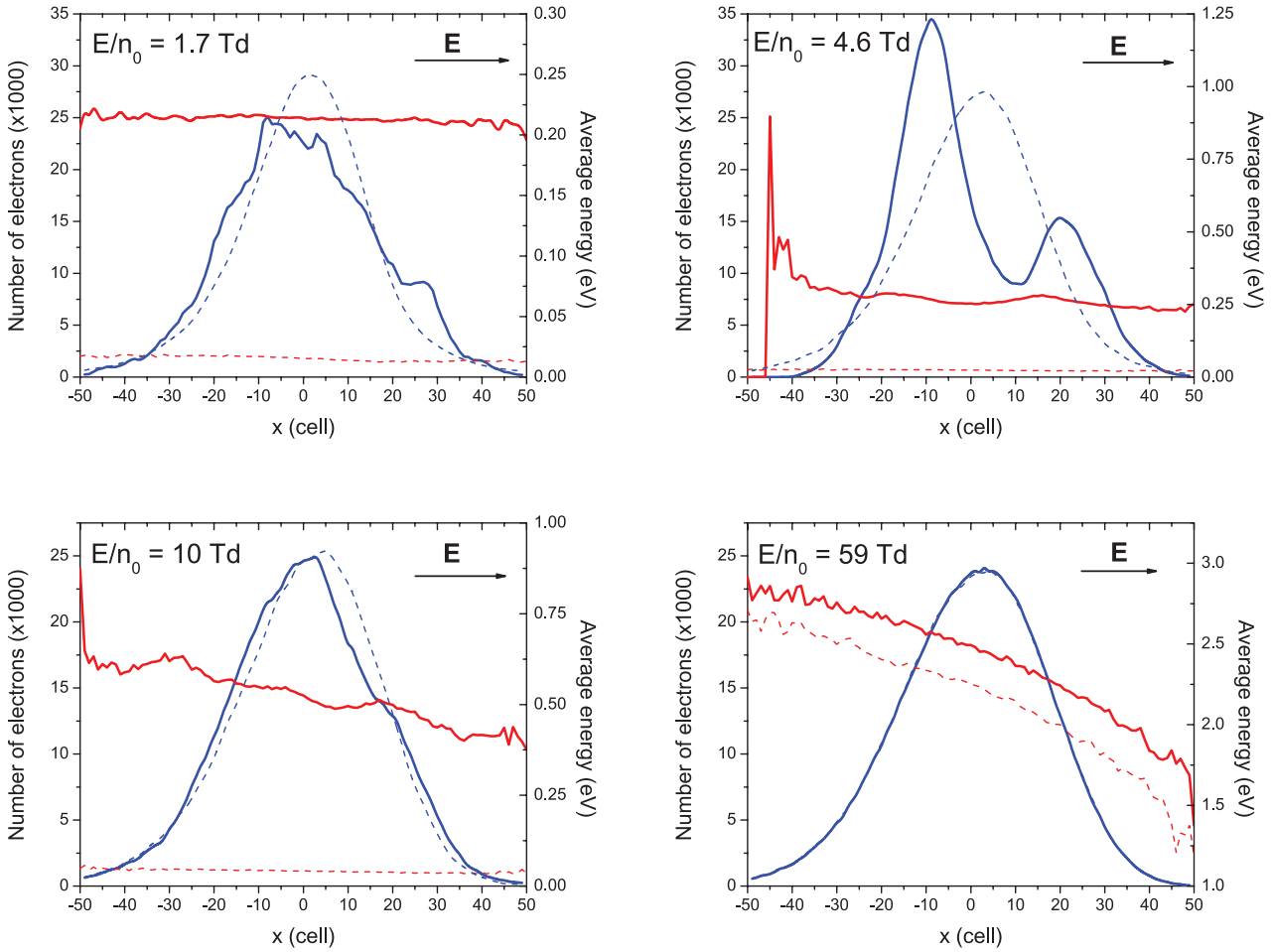

Figure 8. Spatial profile of electrons (blue curves) and spatially resolved averaged energy (red curves) at four different E/n_0 in CF_3I. Full lines denote the results when electron attachment is treated as a non-conservative process, while the dashed lines represent our results when electron attachment is treated as a conservative inelastic process with zero energy loss.

attachment heating while for higher E/n_0 this follows from the explicit effects of ionization. As mentioned above, when transport processes are greatly affected by attachment heating the slower electrons at the back of the swarm are consumed at a faster rate than those at the front of the swarm. Thus, in the case of drift, the electron attachment acts to push the centre of mass forward, increasing the bulk drift velocity above its flux component. For higher E/n_0 when ionization takes place, the ionization rate is higher for faster electrons at the front of the swarm than for slower electrons at the back of the swarm. As a result, electrons are preferentially created at the front of the swarm which results in a shift in the centre of mass. Of course, this physical picture is valid if collision frequency for ionization is an increasing function of electron energy. This is true for electrons in both SF_6 and CF_3I. The explicit effects of electron attachment are much stronger than those induced by ionization. When ionization is dominant non-conservative process, the differences between two sets of data are within 30% for both gases. When attachment dominates ionization, however, then the discrepancy between two sets of data might be almost two orders of magnitude, as for electrons in SF_6 in the limit of the lowest E/n_0.

The flux drift velocity is a monotonically increasing function of E/n_0 while the bulk component behaves in a qualitatively different fashion. A prominent feature of electron drift in SF_6 and CF_3I is the presence of a very strong NDC in the profile of the bulk drift velocity. On the other hand, a decrease in the flux drift velocity with increasing E/n_0 has not been observed. Such behavior is similar of the recently observed NDC effect for positrons in molecular gases [78, 79] where Positronium (Ps) formation plays the role of electron attachment.

In order to provide physical arguments for an explanation of NDC in the bulk drift velocity, in figure 8 we show the spatial profile and spatially resolved average energy of electrons in CF_3I. Calculations are performed for four different values of E/n_0 as indicated in the graph. The direction of the applied electric field is also shown. Two fundamentally different scenarios are discussed: (1) the electron attachment is treated as a conservative inelastic process with zero energy loss, and (2) the electron attachment is treated regularly, as a true non-conservative process. The first scenario is made with the aim of illustrating that NDC is not primarily caused by the shape of cross section for attachment but rather by the synergism of explicit and the implicit effects of the number changing nature of the process on electron transport. Sampling of spatially resolved data in our Monte Carlo simulations is performed using the continuous rescaling. The continuous rescaling produces smoother curves and in most cases it is more reliable

as compared to the discrete rescaling and swarm duplication. The results of the first scenario are presented by dashed lines while the second scenario where electron attachment is treated as a true non-conservative process, is represented by full lines.

When electron attachment is treated as a conservative inelastic process, the spatial profile of electrons has a well defined Gaussian profile with a small bias induced by the effect of electric field. The non-symmetrical feature of spatial profile is further enhanced with increasing E/n_0. While for lower E/n_0 the spatial variation of the average energy is relatively low, for higher E/n_0, e.g. for E/n_0 of 59 Td the slope of the average energy is quite high, indicating that the electron swarm energy distribution is normally spatially anisotropic. It is important to note that there are no imprinted oscillations in the spatial profile of the electrons or in the profile of the average energy which is a clear sign that the collisional energy loss is governed essentially by 'continuous' energy loss processes [32].

When electron attachment is treated as a true non-conservative process, the spatial profile and the average energy of electrons are drastically changed. For all considered reduced electric fields spatially resolved average energy is greater as compared to the case when electron attachment is treated as a conservative inelastic process. For E/n_0 of 1.7 and 4.6 Td the spatial profiles of electrons depart from a typical Gaussian shape. For 1.7 Td there is very little spatial variation in the average energy along the swarm. When $E/n_0 = 4.6$ Td, however, the spatial profile is skewed, asymmetric and shifted to the left. This shift corresponds approximately to the difference between bulk drift velocities in the two scenarios. We observe that the trailing edge of the swarm is dramatically cut off while the average energy remains essentially unaltered. At the leading edge of the swarm, however, we observe a sharp jump in the average energy which is followed by a sharp drop-off. In addition, the height of spatial profile is significantly increased in comparison to the Gaussian profile of the swarm when electron attachment is treated as a conservative inelastic process. For higher E/n_0 the signs of explicit effects of electron attachment are still present but are significantly reduced. For $E/n_0 = 10$ Td the spatial dependence of the average energy is almost linear with a small jump at the leading edge of the swarm. Comparing trailing edges of the swarms at 4.6 and 10 Td we see that for higher electric field the spatial profile of electrons is by far less cut off. This suggests that for increasing E/n_0 there are fewer and fewer electrons that are consumed by electron attachment. Finally, for $E/n_0 = 59$ Td the spatial profile of electrons is exactly the same as the profile obtained under conditions when electron attachment is treated as a conservative inelastic process.

The spatially resolved attachment rates are displayed in figure 9 and are calculated under the same conditions as for the spatial profile of the electrons and spatially averaged energy. We see that the attachment rate peaks at the trailing edge of the swarm where the average energy of the electrons is lower. Attachment loss of these lower energy electrons causes a forward shift to the swarm centre of mass, with a corresponding increase in the bulk drift velocity. For increasing E/n_0, the spatially resolved attachment rate coefficients are reduced and linearly decrease from the trailing edge towards the leading

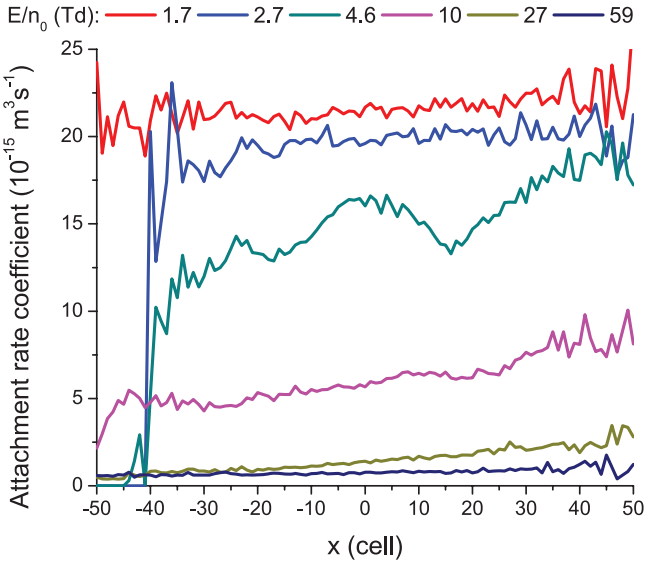

Figure 9. Spatially resolved attachment rate coefficient for a range of E/n_0 as indicated on the graph. Calculations are performed for electrons in CF_3I.

part of the swarm. At the same time the electrons at the leading edge of the swarm have enough energy to undergo ionization. This suggests much less explicit influence of electron attachment on the electron swarm behavior. As a consequence, NDC is removed from the profile of the bulk drift velocity.

In addition to the explicit effects of electron attachment there are implicit effects due to energy specific loss of electrons, which changes the swarm energy distribution as a whole, and thus indirectly changes the swarm flux. Generally speaking, it is not possible to separate the explicit from implicit effects, except by analysis with and without the electron attachment. Using these facts as motivational factors, in figure 10 we show the electron energy distribution functions for the same four values of E/n_0 considered above. The electron energy distribution functions are calculated when electron attachment is treated as a true non-conservative process (full line) and under conditions when electron attachment is assumed to be a conservative inelastic process (dashed line). As for electrons in SF_6, we observe a 'hole burning' effect in the energy distribution function which is certainly one of the most illustrative examples of the implicit effects. Likewise, we see that the high energy tail of the distribution function falls off very slowly even slower than for Maxwellian. Under these circumstances, when the actual distribution function significantly deviates from a Maxwellian, the numerical schemes for solving the Boltzmann equation in the framework of moment methods usually fail. Indeed, for E/n_0 less than approximately 20 Td we have found a sudden deterioration in the convergence of the transport coefficients which was most pronounced for the bulk properties. Furthermore, we see that the 'hole burning' effect is not present when electron attachment is treated as a conservative inelastic process. The lower energy part of the distribution function is well populated while high energy part falls off rapidly. For increasing E/n_0 and when electron attachment is treated as a true non-conservative process, the effect of hole burning is reduced markedly while

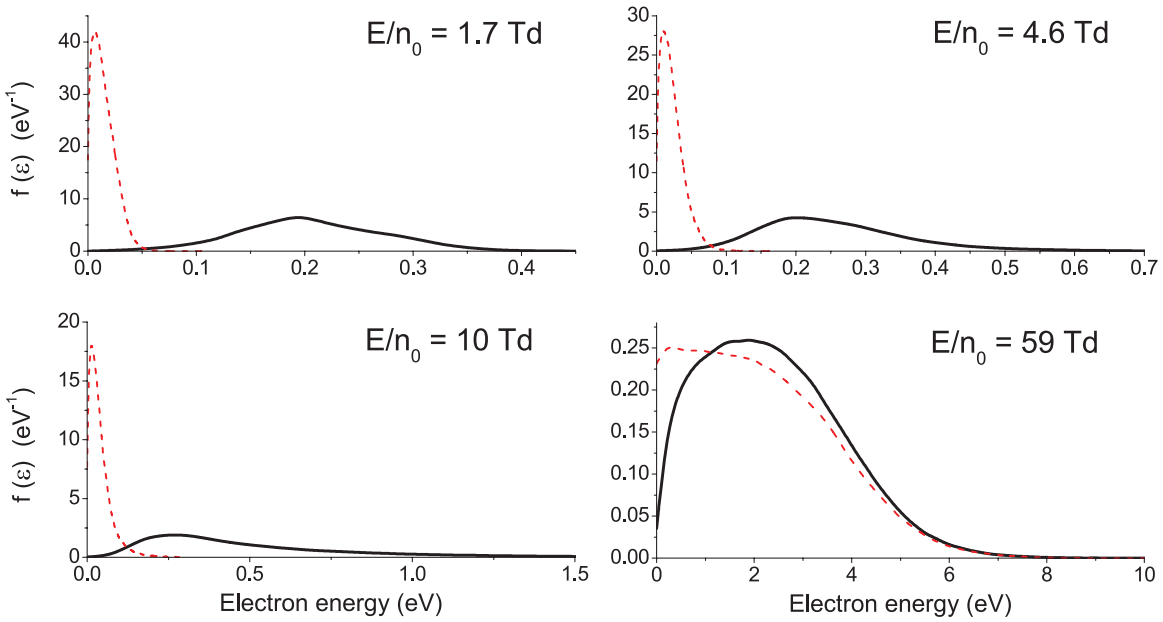

Figure 10. Energy distribution functions for four different E/n_0 for electrons in CF_3I. Black lines denote the results when electron attachment is treated as non-conservative process while dashed red lines represent our results when electron attachment is treated as a conservative inelastic process.

the high energy part of the distribution function coincides with the corresponding one when electron attachment is treated as a conservative inelastic process.

Before embarking on a discussion of our results for diffusion coefficients, one particular point deserves more mention. NDC phenomenon in the bulk drift velocity has not been experimentally verified, neither for SF_6 nor for CF_3I. On the other hand, as we have already seen, the two entirely different theoretical techniques for calculating the drift velocity predict the existence of the phenomenon. Thus, it would be very useful to extend the recent measurements of the drift velocity in both SF_6 and CF_3I to lower E/n_0 with the aim of confirming the existence of NDC. On the other hand, such measurements are most likely very difficult, even impossible due to rapid losses of electron density in experiment.

3.1.3. Diffusion coefficients. Variations of the longitudinal and transverse diffusion coefficients with E/n_0 for electrons in SF_6 are displayed in figures 11 and 12, respectively. From the E/n_0-profiles of the longitudinal and transverse flux diffusion coefficients, we observe that different rescaling procedures for Monte Carlo simulations agree very well. For the bulk components, the agreement is also very good for intermediate and higher E/n_0 and only in the limit of the lowest E/n_0 the agreement is deteriorated. Over the range of E/n_0 considered we see that there is an excellent agreement between continuous and discrete rescaling.

Comparing Monte Carlo and BOLSIG+ results, the deviations are clearly evident. They might be attributed to the inaccuracy of the two term approximation of the Boltzmann equation which is always considerably higher for diffusion than for the drift velocity. For higher E/n_0, inelastic collisions are significant and the distribution function deviates substantially from isotropy in velocity space. In these circumstances,

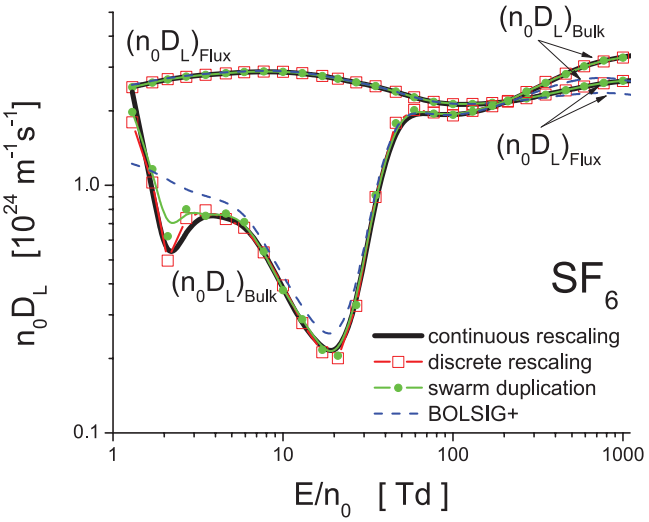

Figure 11. Variation of the longitudinal diffusion coefficient with E/n_0 for electrons in SF_6. Monte Carlo results using three different techniques for electron number density compensation are compared with the BOLSIG+ results.

the two term approximation of the Boltzmann equation fails and multi-term Boltzmann equation analysis is required. For lower E/n_0, however, the role of inelastic collisions is of less significance, but still discrepances between the BOLSIG+ and Monte Carlo results are clearly evident, particularly for the longitudinal diffusion coefficient. This suggests that further analyses of the impact of electron attachment on the distribution function in velocity space of electrons in SF_6 would be very useful.

From the profiles of the longitudinal diffusion coefficient at lower and intermediate values of E/n_0 we observe the following interesting points. In contrast to drift velocity (and transverse diffusion coefficient shown in figure 12) we see

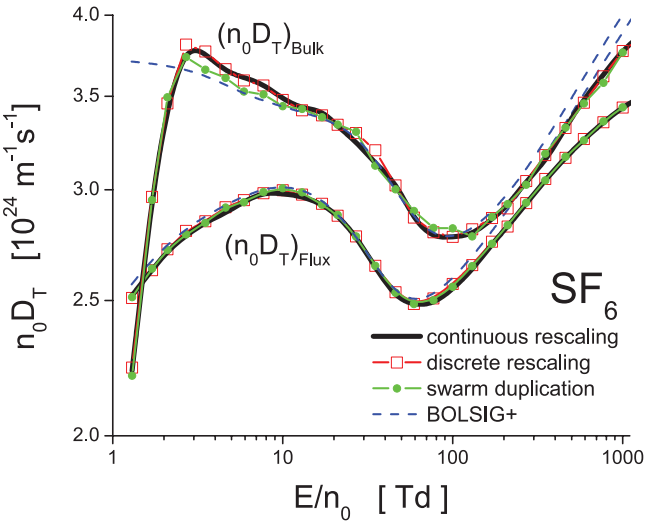

Figure 12. Variation of the transverse diffusion coefficient with E/n_0 for electrons in SF_6. Monte Carlo results using three different techniques for electron number density compensation are compared with the BOLSIG+ results.

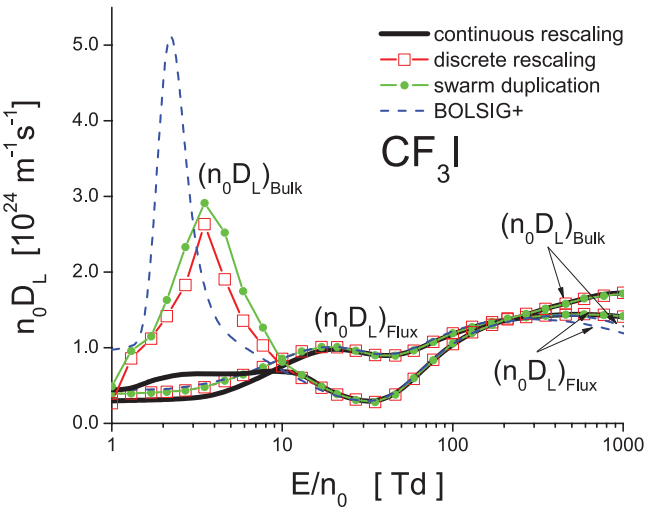

Figure 13. Variation of the longitudinal diffusion coefficient with E/n_0 for electrons in CF_3I. Monte Carlo results using three different techniques for electron number density compensation are compared with the BOLSIG+ results.

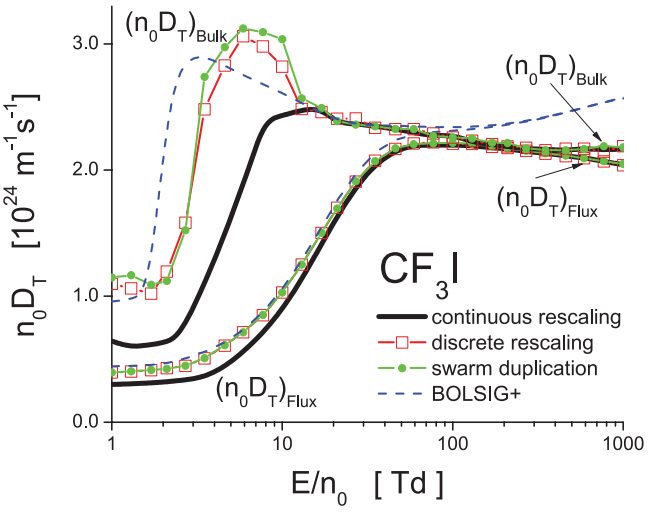

Figure 14. Variation of the transverse diffusion coefficient with E/n_0 for electrons in CF_3I. Monte Carlo results using three different techniques for electron number density compensation are compared with the BOLSIG+ results.

that the bulk diffusion coefficient is smaller than the corresponding flux component. This indicates that the decrease in electron numbers due to attachment weakens diffusion along the field direction. As already discussed, attachment loss of electrons from the trailing edge of the swarm causes a forward shift to the swarm centre of mass, with the corresponding increases in the bulk drift velocity and mean energy. The same effects result in an enhancement of the flux longitudinal diffusion. It should be noted that when attachment heating takes place, the opposite situation (bulk is higher than flux) has also been reported [25]. This is a clear sign that the energy dependence of the cross sections for electron attachment is of primary importance for the analysis of these phenomena. For higher E/n_0, however, where the contribution of ionization becomes important, we observe that the diffusion is enhanced along the field direction, e.g. the bulk dominates the flux. This is always the case if the collision frequency for ionization is an increasing function of the electron energy, independently of the gaseous medium considered.

From the profiles of the transverse diffusion coefficient the bulk values are greater than the corresponding flux values over the range of E/n_0 considered in this work. Only in the limit of the lowest E/n_0 the opposite situation holds: the flux is greater than the bulk. In contrast to the longitudinal diffusion, spreading along the transverse directions is entirely determined by the thermal motion of the electrons. The flux of the Brownian motion through a transverse plane is proportional to the speed of the electrons passing through the same plane. Therefore, the higher energy electrons contribute the most to the transversal expansion, so attachment heating enhances transverse bulk diffusion coefficient.

Figures 13 and 14 show the variations of the longitudinal and transverse diffusion coefficients with E/n_0 for electrons in CF_3I, respectively. From the E/n_0-profiles of the bulk diffusion coefficients we observe an excellent agreement between different rescaling procedures for $E/n_0 > 10$ Td. The same applies for the flux component of the longitudinal diffusion. For $E/n_0 < 10$ Td the agreement is poor for bulk components, particularly between the continuous rescaling from one side and discrete rescaling and/or swarm duplication from the other side. The agreement is better for the flux components.

Comparing Monte Carlo and BOLSIG + results, we see that the maximum error in the two term approximation, for both diffusion coefficients occurs at lower and higher E/n_0. In contrast to SF_6, CF_3I has rapidly increasing cross sections for vibrational excitations in the same energy region where the cross section of momentum transfer in elastic collisions decreases with the electron energy. Under these conditions, the energy transfer is increased and collisions no longer have the effect of randomizing the direction of electron motion. As a consequence, the distribution function deviates significantly from isotropy in velocity space and two term approximation of the Boltzmann equation fails.

When considering the differences between the bulk and flux values of diffusion coefficients the situation is much more complex comparing to SF_6. From the E/n_0-profiles of the longitudinal diffusion coefficient one can immediately see that for lower and higher E/n_0, the bulk is greater than the corresponding flux values while at intermediate E/n_0 the opposite situation holds: the flux is greater than the bulk. The behavior of the transverse diffusion coefficient is less complex, as over the entire of E/n_0 the bulk is greater that the corresponding flux values.

As we have demonstrated, in contrast to drift velocity the behavior and differences between the bulk and flux diffusion coefficients is somewhat harder to interpret. This follows from the complexity of factors which contribute to or influence the diffusion coefficients. The two most important factors are the following: (a) the thermal anisotropy effect resulting from different random electron motion in different directions; and (b) the anisotropy induced by the electric field resulting from the spatial variation of the average energy and local average velocities throughout the swarm which act so as to either inhibit or enhance diffusion. Additional factors include the effects of collisions, energy-dependent total collision frequency, and presence of non-conservative collisions. Couplings of these individual factors are always present and hence sometimes it is hard to elucidate even the basic trends in the behavior of diffusion coefficients. In particular, to understand the effects of electron attachment on diffusion coefficients and associated differences between bulk and flux components, the variation in the diffusive energy tensor associated with the second-order spatial variation in the average energy with E/n_0 should be studied. This remains the program of our future work.

3.1.4. Rate coefficients. In figure 15 we show the variation of steady-state Townsend ionization and attachment coefficients with E/n_0 for electrons in SF_6. The agreement between different rescaling procedures and BOLSIG+ code is very good. It is important to note that the agreement is very good, even in the limit of the lowest E/n_0 considered in this work where the electron energy distribution function is greatly affected by electron attachment. The curves show expected increase in α/n_0 and expected decrease in η/n_0, with increasing E/n_0. The value obtained for critical electric field is 361 Td which is in excellent agreement with experimental measurements of Aschwanden [80].

In figure 16 we show variation of the steady-state Townsend ionization and attachment coefficients with E/n_0 for electrons in CF_3I. The agreement between different rescaling procedure and BOLSIG+ code is excellent for ionization coefficient. From the E/n_0-profile of attachment coefficient, we see that the continuous rescaling slightly overestimates the remaining scenarios of computation. The critical electric field for CF_3I is higher than for SF_6. This fact has been recently used as a motivational factor for a new wave of studies related to the insulation characteristics of pure CF_3I and its mixture with other gases, in the light of the present search for suitable alternatives to SF_6. The value obtained for critical electric field in our calculations is 440 Td which is in close agreement with experimental measurements under steady-state [63, 81]

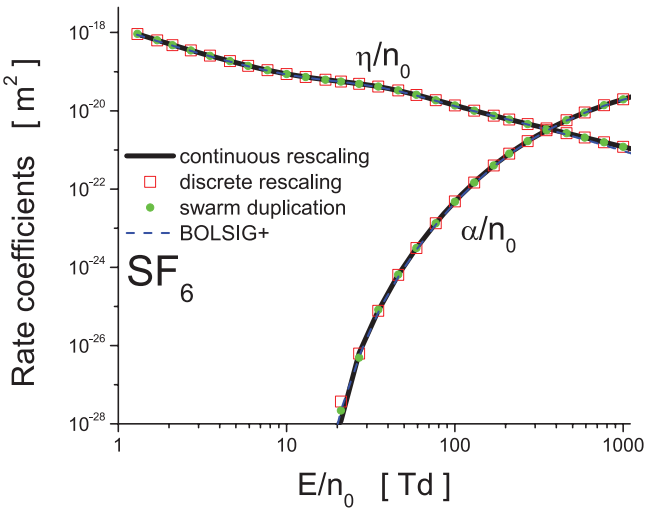

Figure 15. Variation of the rate coefficients with E/n_0 for electrons in SF_6. Monte Carlo results using three different techniques for electron number density compensation are compared with the BOLSIG+ results.

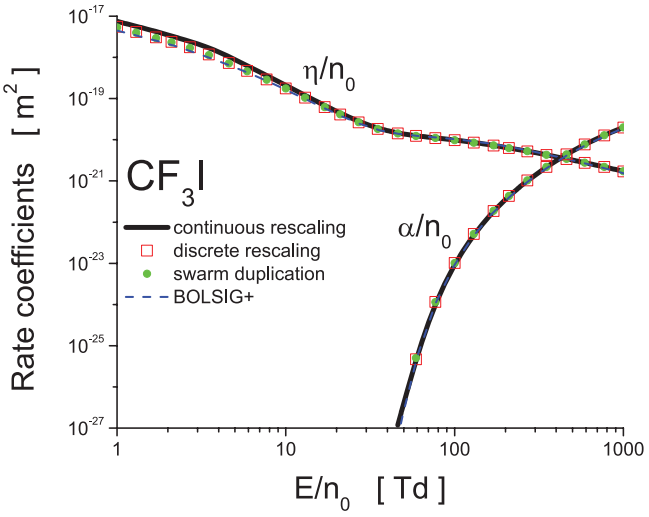

Figure 16. Variation of the rate coefficients with E/n_0 for electrons in CF_3I. Monte Carlo results using three different techniques for electron number density compensation are compared with the BOLSIG+ results.

and pulsed-Townsend [82] conditions, as well as with recent calculations performed by Kawaguchi *et al* [58] and Deng and Xiao [52].

3.2. Recommendations for implementation

In this section, we discuss the main features of the rescaling procedures and we give recommendations on how to use them in future Monte Carlo codes. Based on our experience achieved by simulating the electron transport in SF_6, CF_3I and other attaching gases, we have observed that if correctly implemented the procedures generally agree very well. The agreement between different rescaling procedures is always better for the flux than for the bulk properties. We found a poor agreement for the bulk diffusion coefficients, particularly for the lower E/n_0 while for mean energy, drift velocity and

rate coefficients the agreement is reasonably good. For lower E/n_0 when the distribution function is extremely affected by electron attachment, the agreement between swarm duplication and discrete rescaling is also good. This is not surprising as these two techniques are essentially the same.

In terms of implementation, the Monte Carlo codes can be relatively easily upgraded with the procedures for swarm duplication and/or discrete rescaling. Special attention during the implementation of these procedures should be given to the choice of the length of time steps after which the cloning of the electrons is done. If the length of this time step appears to be too long as compared to the time constant which corresponds to the attachment collision frequency, then the distribution function could be disturbed due to a low statistical accuracy. In other words, depleting certain pockets of the EEDF means that those cannot be recovered at all. On the other hand, if the length of the time steps is too small, the speed of simulation could be significantly reduced. The implementation of the continuous rescaling procedure is somewhat more complicated.

Which procedure is, the most flexible? It is difficult to answer this question because the answer depends on the criteria of flexibility. If the criterion for flexibility is associated with the need for *a priori* estimates which are necessary for setting the simulation, then the technique of continuous rescaling is certainly the most flexible. Once implemented, and thoroughly tested this procedure allows the analysis of electron transport in strongly attaching gases regardless of the energy dependence of the cross section for electron attachment. On the other hand, for the analysis of electron transport in weakly attaching gases, the discrete rescaling is very convenient because it is easier for implementation into the codes and less demanding in terms of the CPU time.

In terms of reliability and accuracy, the comparison of the results obtained for various transport properties using the rescaling procedures for Monte Carlo simulations and the Boltzmann equation codes shows that the rescaling procedures described herein are highly reliable. It should be noted that only the multi term codes for solving the Boltzmann equation may offer the final answer. Restrictions of the TTA for solving the Boltzmann equation were demonstrated many times in the past [7, 31], especially when it comes to the calculations of diffusion coefficients. Testing and benchmarking against other Boltzmann solvers are currently ongoing.

3.3. Experiments in strongly attaching gases: difficulties induced by non-hydrodynamic effects

It must be noted at this point that most processes scale with pressure, so the independence on pressure would be maintained and so would be the equilibration of EEDFs affected by excessive attachment. Most of the processes fall into that category. These processes are best visualized in an infinite uniform environment. Standard swarm experiments are built in such a way that boundaries are not felt over appreciable volume and thus, they mimic hydrodynamic conditions very well. However, going to high E/n_0 requires operating at lower pressures and there the boundaries may be felt over a larger portion of the volume. In general, whenever boundaries of any kind are introduced selective losses resulting in very different mean free paths of different groups of particles may lead to selective losses. The resulting holes in the distribution may be filled in by collisions, so when considerable selective losses are introduced results may become the pressure dependent (even when the cross section is not dependent on the pressure). The same is true for temporal limitations. For example, if the frequency of collisions is small, so that the mean free time is comparable to the time required to accelerate to energies where cross sections decrease with the electron energy, the runaway effects may be developed. Similar effects may be created due to temporal variations of the field that do not allow full equilibration. The pressure dependence of the results will develop under such conditions (and so would the dependence on the size of the vessel). The development of a non-hydrodynamic theory for solving the Boiltzmann equation is difficult and the best solution is a Monte Carlo simulation technique. For that reason, rescaling procedures are essential in modeling of the non-hydrodynamic (non-local) development of charged particle ensembles.

Experiments in gases with a very large attachment (typically at low energies) may be difficult to carry out due to a large loss of electrons. The fact that experiments in diluted gas mixtures of such gases may be feasible, means that cross sections may be obtained. Yet, one should be aware of two main problems. Even in such mixtures and depending on the size of the experiment, attachment may be high enough to induce depletion of the distribution function thus making results pressure dependent or abundance dependent. If one wants to extend the calculations to pure attaching gas for smaller vessels and pressures, one needs to be aware that only techniques that take full non-hydrodynamic description of the swarm development, are required. Similar effects have been observed in gases always associated with strong attachment such as oxygen [76] and water vapor [83]. In any case, the critical effects that include NDC for bulk drift velocity as a result of excessive loss of electrons in attachment can be observed in gases like SF_6 and CF_3I based on hydrodynamic expansion and even based on the two term theory provided that theory takes into account the explicit and implicit non-conservative effects of the attachment.

4. Conclusion

In this paper, we have presented the development, implementation and benchmarking of the rescaling procedures for Monte Carlo simulations of electron transport in strongly attaching gases. The capabilities of the rescaling procedures have been described by systematic investigation of the influence of electron attachment on transport coefficients of electrons in SF_6 and CF_3I. Among many important points, the key results arising from this paper are:

(1) We have presented two distinctively different methods for compensation of electrons in Monte Carlo simulations of electron transport in strongly attaching gases, e.g. the discrete and the continuous procedures. In order to avoid the

somewhat arbitrary choice of the fictitious ionization rate, we have extended the continuous rescaling procedure, initially developed by Li *et al* [61], by introducing a time-dependent collision frequency for the fictitious ionization process.

(2) One of the initial motivating factors for this work was to provide accurate data for transport properties of electrons in SF_6 and CF_3I which are required as input in fluid models of plasma discharges. In this work, for the first time, we have calculated the mean energy, drift velocity and diffusion coefficients as well as rate coefficients for lower E/n_0 for electrons in SF_6 and CF_3I.

(3) We have demonstrated the differences which can exist between the bulk and flux transport coefficients and the origin of these differences. Our study has shown that the flux and bulk transport properties can vary substantially from one another, particularly in the presence of intensive attachment heating. Thus, one of the key messages of this work is that theories which approximate the bulk transport coefficients by the flux are problematic and generally wrong.

(4) We have demonstrated and interpreted physically the phenomenon of the anomalous behavior of the mean energy of electrons in SF_6, in which the mean energy is reduced for increasing E/n_0. The phenomenon was associated with the interplay between attachment heating an inelastic cooling. The same phenomenon has not been observed for electrons in CF_3I indicating that the role of the cross sections is vital.

(5) We have explained and identified a region of NDC in the bulk drift velocity, originating from the explicit influence of electron attachment. The phenomenon has been explained using the concept of spatially-resolved transport properties along the swarm.

(6) The publicly available two term Boltzmann solver, BOLSIG+, has been shown to be accurate for calculations of mean energy, drift velocity and rate coefficients for electrons in SF_6 and CF_3I. On the other hand, significant differences between our Monte Carlo and BOLSIG+ results for diffusion coefficients have been observed, particularly for electrons in CF_3I in the limit of the lowest E/n_0 considered in this work.

Various rescaling procedures for Monte Carlo simulations described in this work have recently been applied to modeling of electron transport in strongly attaching gases under the influence of time-dependent electric and magnetic fields. It will be challenging to investigate the synergism of magnetic fields and electron attachment in radio-frequency plasmas. Likewise, the remaining step to be taken, is to apply the rescaling procedures presented in this work to investigate the influence of positronium formation on the positron transport properties. This remains the focus of our future investigation. Finally, we hope that this paper will stimulate further discussion on methods of correct representation of the effects induced by electron attachment on transport properties of electrons in strongly attaching gases.

Acknowledgments

The authors acknowledge support from MPNTRRS Projects OI171037 and III41011.

References

[1] Christophorou L G and Olthoff J K 2004 *Fundamental Electron Interactions with Plasma Processing Gases* (New York: Springer)
[2] Makabe T and Petrović Z Lj 2014 *Plasma Electronics: Applications in Microelectronic Device Fabrication* (New York: CRC Press)
[3] Christophorou L G and Pinnaduwage L A 1990 *IEEE Trans. Electr. Insul.* **25** 55
[4] Rolandi L, Riegler W and Blum W 2008 *Particle Detection with Drift Chambers* (Berlin: Springer)
[5] Sauli F 2014 *Gaseous Radiation Detectors* (Cambridge: Cambridge University Press)
[6] Bošnjaković D, Petrović Z Lj, White R D and Dujko S 2014 *J. Phys. D: Appl. Phys.* **47** 435203
[7] Petrović Z Lj, Dujko S, Marić D, Malović G, Nikitović Ž, Šašić O, Jovanović J, Stojanović V and Radmilović-Radjenović M 2009 *J. Phys. D: Appl. Phys.* **42** 194002
[8] Petrović Z Lj, Šuvakov M, Nikitović Ž, Dujko S, Šašić O, Jovanović J, Malović G and Stojanović V 2007 *Plasma Sources Sci. Technol.* **16** S1
[9] Huxley L G H and Crompton R W 1974 *The Drift and Diffusion of Electrons in Gases* (New York: Wiley)
[10] Christophorou L G, McCorkle D L and Anderson V E 1971 *J. Phys. B: At. Mol. Phys.* **4** 1163
[11] Phelps A V and van Brunt R J 1988 *J. Appl. Phys.* **64** 4269
[12] Christophorou L G and Olthoff J K 2000 *J. Phys. Chem. Ref. Data* **29** 267
[13] Jarvis G K, Kennedy R A and Mayhew C A 2001 *Int. J. Mass Spectrom.* **205** 253
[14] Dahl D A and Franck C M 2013 *J. Phys. D: Appl. Phys.* **46** 445202
[15] Rabie M, Haefliger P, Chachereau A and Franck C M 2015 *J. Phys. D: Appl. Phys.* **48** 075201
[16] Hunter S R and Christophorou L G 1984 *J. Chem. Phys.* **80** 6150
[17] Novak J P and Frechette M F 1988 *J. Appl. Phys.* **63** 2570
[18] Hunter S R, Carter J G and Christophorou L G 1988 *Phys. Rev.* A **38** 58
[19] Petrović Z Lj, Wang W C and Lee L C 1988 *J. Appl. Phys.* **64** 1625
[20] Petrović Z Lj, Wang W C, Suto M, Han J C and Lee L C 1990 *J. Appl. Phys.* **67** 675
[21] Raju G G 2006 *Gaseous Electronics: Theory and Practice* (New York: CRC Press)
[22] Raju G G 2012 *Gaseous Electronics: Tables, Atoms, and Molecules* (New York: CRC Press)
[23] Cavalleri G 1969 *Phys. Rev.* **179** 186
[24] Petrović Z Lj and Crompton R W 1985 *J. Phys. B: At. Mol. Phys.* **17** 2777
[25] Ness K F and Robson R E 1986 *Phys. Rev.* A **34** 2185
[26] Nolan A M, Brennan M J, Ness K F and Wedding A B 1997 *J. Phys. D: Appl. Phys.* **30** 2865
[27] Dujko S, Raspopović Z M, Petrović Z Lj and Makabe T 2003 *IEEE Trans. Plasma Sci.* **31** 711
[28] White R D, Robson R E and Ness K F 1999 *Phys. Rev.* E **60** 7457
[29] Dujko S, Ebert U, White R D and Petrović Z Lj 2011 *Japan J. Appl. Phys.* **50** 08JC01
[30] Robson R E 1991 *Aust. J. Phys.* **44** 685

[31] White R D, Robson R E, Dujko S, Nicoletopoulos P and Li B 2009 *J. Phys. D: Appl. Phys.* **42** 194001
[32] Dujko S, White R D, Raspopović Z M and Petrović Z Lj 2012 *Nucl. Instrum. Methods Phys. Res.* B **279** 84
[33] Robson R E, White R D and Petrović Z Lj 2005 *Rev. Mod. Phys.* **77** 1303
[34] Dujko S, Markosyan A H, White R D and Ebert U 2013 *J. Phys. D: Appl. Phys.* **46** 475202
[35] Markosyan A H, Dujko S and Ebert U 2013 *J. Phys. D: Appl. Phys.* **46** 475203
[36] Bletzinger P 1990 *J. Appl. Phys.* **67** 130
[37] Stoffels E, Stoffelsd W, Venderm D, Haverlaag M, Kroesen G M W and de Hoog F J 1995 *Contrib. Plasma Phys.* **35** 331
[38] Chabert P and Sheridan T E 2000 *J. Phys. D: Appl. Phys.* **33** 1854
[39] Kono A 2002 *Appl. Surf. Sci.* **192** 115
[40] Zhao S X, Gao F, Wang Y N and Bogaerts A 2012 *Plasma Sources Sci. Technol.* **21** 025008
[41] Chabert P, Lichtenberg A J, Lieberman M A and Marakhtanov A M 2003 *J. Appl. Phys.* **94** 831
[42] Robson R E 1986 *J. Chem. Phys.* **85** 4486
[43] Vrhovac S B and Petrović Z Lj 1996 *Phys. Rev.* E **53** 4012
[44] Yousfi M, Segur P and Vassiliadis T 1985 *J. Phys. D: Appl. Phys.* **18** 359
[45] Itoh H, Miurat Y, Ikuta N, Nakao Y and Tagashira H 1988 *J. Phys. D: Appl. Phys.* **21** 922
[46] Itoh H, Kawaguchi M, Satoh K, Miura Y, Nakano Y and Tagashira H 1990 *J. Phys. D: Appl. Phys.* **23** 299
[47] Itoh H, Matsumura T, Satoh K, Date H, Nakano Y and Tagashira H 1993 *J. Phys. D: Appl. Phys.* **26** 1975
[48] Frechette M F and Novak J P 1987 *J. Phys. D: Appl. Phys.* **20** 438
[49] Pinheiro M J and Loureiro J 2002 *J. Phys. D: Appl. Phys.* **35** 3077
[50] Tezcan S S, Akcayol M A, Ozerdem O C and Dincer M S 2010 *IEEE Trans. Plasma Sci.* **38** 2332
[51] Li X, Zhao H, Wu J and Jia S 2013 *J. Phys. D: Appl. Phys.* **46** 345203
[52] Deng Y and Xiao D 2014 *Japan J. Appl. Phys.* **53** 096201
[53] Dujko S, White R D, Petrović Z Lj and Robson R E 2010 *Phys. Rev.* E **81** 046403
[54] Yousfi M, Hennad A and Alkaa A 1994 *Phys. Rev.* E **49** 3264
[55] Dincer M S and Gaju G R 1983 *J. Appl. Phys.* **54** 6311
[56] Dincer M S, Ozerdem O C and Bektas S 2007 *IEEE Trans. Plasma Sci.* **35** 1210
[57] Satoh K, Itoh H, Nakano Y and Tagashira H 1988 *J. Phys. D: Appl. Phys.* **21** 931
[58] Kawaguchi S, Satoh K and Itoh H 2014 *Eur. Phys. J.* D **68** 100
[59] Rapopović Z M, Sakadžić S, Bzenić S and Petrović Z Lj 1999 *IEEE Trans. Plasma Sci.* **27** 1241
[60] Dyatko N A and Napartovich A P 1999 *J. Phys. D: Appl. Phys.* **32** 3169
[61] Li Y M, Pitchford L C and Moratz T J 1989 *Appl. Phys. Lett.* **54** 1403
[62] Mirić J, Šašić O, Dujko S and Petrović Z Lj 2014 *Proc. 27th Summer School and Int. Symp. on the Physics of Ionized Gases (Belgrade)* (Belgrade: Institute of Physics) p 122
[63] Kimura M and Nakamura Y 2010 *J. Phys. D: Appl. Phys.* **43** 145202
[64] Mirić J, de Urquijo J, Bošnjaković D, Petrović Z Lj and Dujko S 2016 *Plasma Sources Sci. Technol.* submitted
[65] Ristivojević Z and Petrović Z Lj 2012 *Plasma Sources Sci. Technol.* **21** 035001
[66] Dujko S, White R D and Petrović Z Lj 2008 *J. Phys. D: Appl. Phys.* **41** 245205
[67] Petrović Z Lj, Raspopović Z, Dujko S and Makabe T 2002 *Appl. Surf. Sci.* **192** 1
[68] Hagelaar G J M and Pitchford L C 2005 *Plasma Sources Sci. Technol.* **14** 722
[69] Kline L and Siambis J 1972 *Phys. Rev.* A **5** 794
[70] Kunhardt E and Tzeng Y 1986 *J. Comput. Phys.* **67** 279
[71] Gallagher J W, Beaty E C, Dutton J and Pitchford L C 1983 *J. Phys. Chem. Ref. Data* **12** 109
[72] Morrow R 1986 *IEEE Trans. Plasma Sci.* **PS-14** 234
[73] Ness K F and Makabe T 2000 *Phys. Rev.* E **62** 4083
[74] White R D, Robson R E, Ness K F and Makabe T 2005 *J. Phys. D: Appl. Phys.* **38** 997
[75] Skullerud H R 1983 *Aust. J. Phys.* **36** 845
[76] McMahon D R A and Crompton R W 1983 *J. Chem. Phys.* **78** 603
[77] Hegerberg R and Crompton R W 1983 *Aust. J. Phys.* **36** 831
[78] Banković A, Dujko S, White R D, Marler J P, Buckman S J, Marjanović S, Malović G, Garcia G and Petrović Z Lj 2012 *New J. Phys.* **14** 035003
[79] Banković A, Dujko S, White R D, Buckman S J and Petrović Z Lj 2012 *Nucl. Instrum. Methods* B **279** 92
[80] Aschwanden Th 1984 *Gaseous Dielectrics* IV ed L G Christophorou and M O Pace (New York: Pergamon) p 24
[81] Hasegawa H, Date H, Shimozuma M and Itoh H 2009 *Appl. Phys. Lett.* **95** 101504
[82] de Urquijo J, Juarez A M, Basurto E and Hernandez-Avila J L 2007 *J. Phys. D: Appl. Phys.* **40** 2205
[83] Robson R E, White R D and Ness K F 2011 *J. Chem. Phys.* **134** 064319